

# Electromagnetic Actuator Modelling with the Extended Modelica Magnetic Library

Thomas Bödrich

Dresden University of Technology, Institute of Electromechanical and Electronic Design  
01062 Dresden, Germany  
Thomas.Boedrich@mailbox.tu-dresden.de

## Abstract

Recently, an improved and extended version of a Modelica library for lumped network modelling of electromagnetic devices has been released [1]. This library is intended for both rough design of the magnetic circuit of those devices as well as for their system simulation. Improvements compared to a first realisation of this library [2] will be discussed and utilization of the extended library for modelling of electromagnetic actuators will be illustrated. To support the work with this library, focus will be on newly-implemented features and on peculiarities of lumped network modelling of electromagnetic actuators rather than on an introductory explanation of the underlying concept of magnetic flux tubes.

*Keywords:* lumped magnetic network; electromagnetic/electrodynamic actuator; system design

## 1 Introduction

The well-established concept of magnetic flux tubes enables the modelling of magnetic fields with lumped networks. In the decades prior to the broad availability of software packages based on finite element techniques, this was the only efficient means for model-based design of the magnetic circuit of electromagnetic devices such as transformers, motors and electromagnetic or electrodynamic actuators. The method of magnetic flux tubes, its utilization for the design of electromagnetic devices as well as derivation of the permeance of many flux tube shapes are explained in-depth for example in [3], [4] and [5] and in condensed form in the documentation of [1].

Even though finite element techniques allow for more accurate calculation of magnetic fields, lumped magnetic network models are still an efficient means for initial rough design of electromagnetic devices and for simulation of their dynamic behaviour during system design. This is due to the relatively little ef-

fort needed for creation of *rough* magnetic network models and to the low computational effort for dynamic simulation compared to finite element techniques.

A first realisation of a Modelica library for lumped network modelling of electromagnetic devices was presented in [2]. This library was improved and extended and is now available [1]. Some of the important improvements of the extended library compared to the prior version are:

- a more general approach for calculation of magnetic reluctance forces (section 2),
- redesigned and extended components for representation of typical flux tube shapes (section 2),
- additional soft magnetic and permanent magnetic materials (section 3),
- more accurate modelling of magnetic leakage fields for *dynamic* simulation by splitting of the magnetomotive force imposed by a coil into separate sources (section 4) and
- additional examples of different modelling depths.

## 2 Reluctance Force Calculation

Generally, the thrust  $F$  developed by a translatory electro-magneto-mechanical actuator (similar for the rotational case with torque and angular position) is equal to the change of magnetic co-energy  $W_m^*$  with armature position  $x$  according to

$$F = \frac{\partial}{\partial x} \int_{(i)} \Psi di = \frac{\partial}{\partial x} W_m^* \quad (1)$$

( $\Psi$  flux linkage,  $i$  actuator current) [4]. In lumped magnetic network models, the above equation simplifies to

$$F = \frac{1}{2} \sum_{i=1}^{n_{linear}} V_{mag i}^2 \frac{dG_{mi}}{dx} \quad (2)$$

where  $n_{linear}$  is the number of flux tube elements with constant relative permeability that change their per-

meance  $G_{m_i}$  with armature position (index  $i$ ),  $V_{mag_i}$  the magnetic voltage across each respective flux tube and  $dG_{m_i}/dx$  the derivative of the respective permeances with respect to armature position. Transition from the general formula based on magnetic co-energy (Eq. (1)) to Eq. (2) is outlined in [4] for the reciprocal of the permeance, i.e. for the magnetic reluctance. Compared to the reluctance force calculation with *Maxwell's* formula used in [2], the newly-implemented approach according to Eq. (2) simplifies force calculation for air gaps different from a simple cylindrical or prismatic shape with axial magnetic flux (see below).

The usability of Eq. (2) is not restricted solely to network models with constant relative permeabilities  $\mu_r$  of the flux tubes. However, it is required that flux tubes with a dependency of the permeability on the flux density  $B$  such as ferromagnetic components with non-linear characteristics  $\mu_r(B)$  do not change their shape with armature motion (e.g. portion of a solenoid plunger where the magnetic flux passes through in axial direction). This limitation is not a strong one, since the permeance of non-linear, high permeable ferromagnetic flux tube elements and its change with armature position compared to that of air gap flux tubes can be neglected in most cases. Because of this constraint, the dimensions of possibly non-linear flux tube elements in sub-package `FluxTube.FixedShape` are fixed, whereas the dimension  $l$  in direction of motion of the linear flux tube elements in sub-package `FluxTube.Force` can vary during simulation. Elements with fixed shape are intended e.g. for modeling of transformer cores or ferromagnetic sections of actuators. Force elements are to be used for modelling of working air gaps or for moving permanent magnets of actuators.

In order to fulfill Eq. (2) in a magnetic network model of a translatory actuator, the reluctance force  $F_m$  of each flux tube with force generation is calculated in the respective element accordingly:

$$F_m = \frac{1}{2} V_{mag}^2 \frac{dG_m}{dx} \quad (3)$$

$V_{mag}$  denotes the magnetic voltage across the flux tube and  $dG_m/dx$  is the derivative of flux tubes permeance  $G_m$  with respect to armature position  $x$ . Summation of all particular reluctance forces to the actuators net force  $F$  according to Eq. (2) is induced by connecting the translatory flange connectors of all flux tube elements with force generation in an actuator model (see example in Figure 4b).

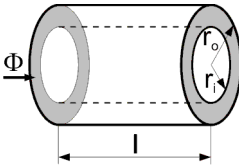
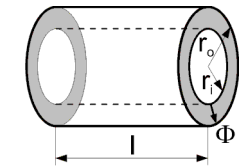
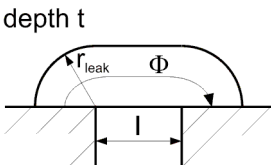
In a particular actuator model, the derivative  $dG_m/dx$  of the models flux tubes with force generation and hence the sign of the generated reluctance force de-

pends on the design of the actuators magnetic circuit and on the definition of the armature coordinate  $x$ . To cover all possible conditions in a uniform way, the above derivative is calculated as follows for all flux tubes with force generation of sub-package `FluxTube.Force`:

$$\frac{dG_m}{dx} = \frac{dG_m}{dl} \frac{dl}{dx} \quad (4)$$

For the flux tubes defined in this package with their rather simple shapes, the derivative  $dG_m/dl$  is given analytically (Table 1).  $l$  is the flux tube dimension that changes with armature motion.  $dl/dx$  is an integer parameter that must be set to +1 or -1 according to the magnetic circuit and the definition of the armature coordinate  $x$  of an actuator. For more complex shapes and variations of dimensions with armature motion, the derivative  $dG_m/dl$  must be provided analytically during model development, preferably by extending the partial model `FluxTube.Force.PartialForce`.

Table 1: Selected flux tube elements with reluctance force generation (subset of `FluxTube.Force`), permeance  $G_m$  and analytic derivative  $dG_m/dl$

(Hollow) cylinder with axial magnetic flux	
	$G_m = \frac{\mu_0 \mu_r A}{l}$ $\frac{dG_m}{dl} = -\frac{\mu_0 \mu_r A}{l^2}$ <p>with <math>A = \pi(r_o^2 - r_i^2)</math></p>
Hollow cylinder with radial magnetic flux	
	$G_m = \frac{\mu_0 \mu_r 2 \pi l}{\ln(r_o/r_i)}$ $\frac{dG_m}{dl} = \frac{\mu_0 \mu_r 2 \pi}{\ln(r_o/r_i)}$
Simple leakage flux tube around cylindrical or prismatic poles	
	$G_m = \frac{2 \mu_0 t}{\pi} \ln\left(1 + \frac{\pi r_{leak}}{2 l}\right)$ $\frac{dG_m}{dl} = -\frac{\mu_0 t r_{leak}}{l^2 \left(1 + \frac{\pi r_{leak}}{2 l}\right)}$

The leakage flux tube shown in Table 1 provides a simple but efficient means to account for leakage around prismatic or cylindrical poles. In the latter case, depth  $t$  is equal to the circumference of a circle given by the average radius of the flux tube. Due to the constant radius  $r_{leak}$  of the leakage field, the model is rather simple. In reality,  $r_{leak}$  is approximately constant for air gap lengths  $l$  greater than this radius, but decreases with air gap lengths less than  $r_{leak}$ . This decrease for small air gaps is neglected in the model since the influence of the leakage flux tube compared to that of the enclosed main air gap (connected in parallel, see example in Figure 4b) decreases for decreasing air gap length  $l$ .

The sub-package `FluxTube.Leakage` contains flux tube shapes typical for leakage flux around prismatic or cylindrical poles that do not change their shape with armature motion. Hence, the permeance of these flux tubes does not depend on armature position and these elements do not contribute to the thrust of a reluctance actuator.

### 3 Modelling of Magnetic Materials

#### 3.1 Soft Magnetic Materials

The characteristics of the relative magnetic permeability versus flux density  $\mu_r(B)$  of various steels, electric sheets (Figure 1) and high permeable materials are included in `Material.SoftMagnetic`. These characteristics are uniformly approximated with a function adapted from [6]:

$$\mu_r = 1 + \frac{\mu_i - 1 + c_a B_N}{1 + c_b B_N + B_N^n} \quad \text{with} \quad B_N = \left| \frac{B}{B|_{\mu_r=\mu_{\max}}} \right|. \quad (5)$$

This approach assures proper behaviour throughout the complete range of flux density. Overshoot and extrapolation errors especially at high flux densities as possible with spline interpolation or with the Modelica Standard Library's table interpolation with continuous derivative can not occur with properly chosen parameters. Two of the five parameters of Eq. (5) have a physical meaning, namely the initial relative permeability  $\mu_i$  at  $B=0$  and the magnetic flux density at maximum permeability  $B|_{\mu_r=\mu_{\max}}$ . Addition of new soft magnetic materials requires determination of the function parameters with a non-linear curve fit outside of the library. For the included materials, attention was paid to accurate fits of  $\mu_r$  for data points at high flux densities ( $B > 0.8$  T). This is because of the large influence of saturated ferromagnetic materials on the behaviour

of a device. It must be noted that a measured characteristics  $\mu_r(B)$  strongly depends on the shape, machining state and heat treatment of a sample, and on the measurement conditions. Hence, different characteristics are possible for similar materials as Figure 1 indicates.

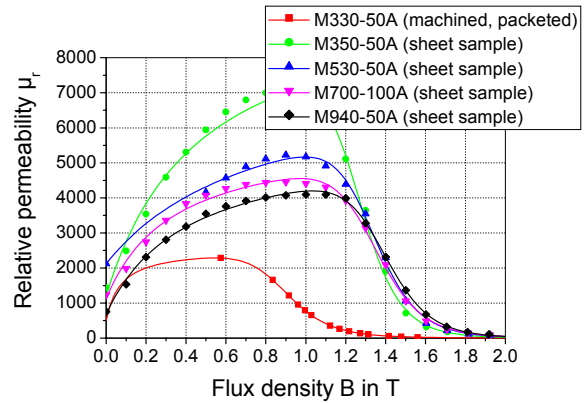


Figure 1: Approximated magnetization characteristics (solid lines) and original data points of included electric sheet materials (all valid for 50 Hz)

Magnetization characteristics that are simulated with Eq. (5) are shown for an electric sheet as an example in the familiar form of flux density vs. field strength  $B(H)$  in Figure 2.

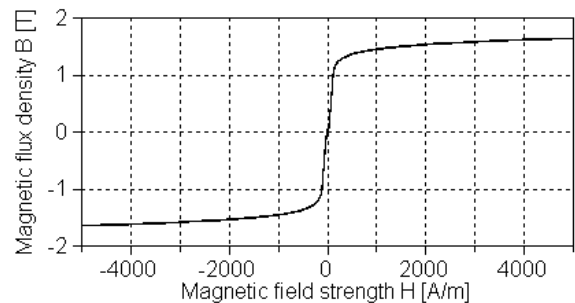


Figure 2: Simulated magnetic flux density vs. magnetic field strength  $B(H)$  of electric sheet M350-50A

#### 3.2 Hard Magnetic Materials

For common permanent magnetic materials, typical values for remanence  $B_{r\ ref}$  and coercivity  $H_{cB\ ref}$  at a reference temperature  $T_{ref}$  and the temperature coefficient  $\alpha_{Br}$  of remanence are provided in sub-package `Material.HardMagnetic` (Figure 3). Records for additional materials can be defined as needed.

Linear demagnetization curves are modelled. The characteristic, temperature-dependent "knee" of many permanent magnetic materials is not considered, since proper design of permanent magnetic cir-

circuits should avoid operation of permanent magnets "below" that point due to partial demagnetization. As a result, the temperature coefficient of coercivity is not considered. Only the temperature coefficient of remanence  $\alpha_{Br}$  is accounted for, since this describes the dependency of the demagnetization curve on the temperature sufficiently for the region "above the knee-point". Remanence  $B_r$  and coercivity  $H_{cB}$  that are effective at a given operating temperature  $T$  are calculated according to

$$B_r = B_{r,ref}(1 + \alpha_{Br}(T - T_{ref})), \quad (6a)$$

$$H_{cB} = H_{cB,ref}(1 + \alpha_{Br}(T - T_{ref})) \quad (6b)$$

in the model `Material.HardMagnetic.PermanentMagnetBehaviour`. Thus, the demagnetization curves shown in Figure 3 are shifted depending on the operating temperature  $T$  and the temperature coefficient of remanence  $\alpha_{Br}$ . Usage of the above-mentioned component and modelling of a permanent magnet are demonstrated in the library in `Examples.ElectrodynamicalActuator.MagneticCircuitModel` (Figure 9).

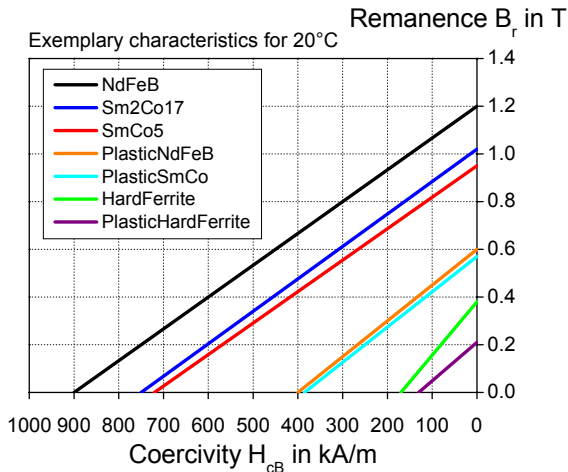


Figure 3: Modelled demagnetization characteristics of included common permanent magnetic materials

## 4 Modelling of Electromagnetic Actuators

As an example of a reluctance actuator, a simple axisymmetric lifting magnet with planar end planes of armature and pole is modelled in sub-package `Examples.ElectromagneticActuator` of the library. Two lumped magnetic network models of different modelling depth are included. In a `SimpleSolenoidModel`, radial leakage that is typical for tubular reluctance actuators is neglected. Higher

accuracy can be gained from an `AdvancedSolenoidModel` in which the coil-imposed magnetomotive force (mmf) is split into two separate mmf sources and the radial leakage flux between armature and yoke is accounted for with leakage permeance  $G_{mLeakRad}$  (Figure 4). This leakage affects the static force-stroke characteristic and the inductance of an actuator and hence its dynamic behaviour especially at large air gaps, as discussed below.

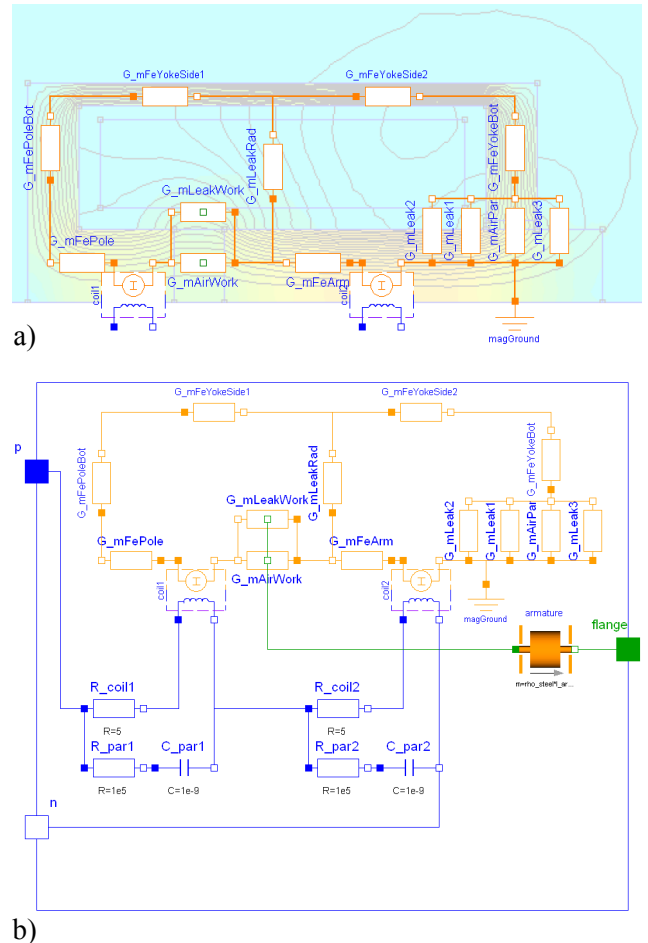


Figure 4: *Magnetic network model of an exemplary solenoid actuator: a) Permeances superimposed on FEA field plot (half-section) for illustration; b) Complete actuator model including electrical subsystem*

Simulation of lumped magnetic network models with multiple mmf sources is easily possible for the stationary case where the coupling between the electrical and the magnetic domain according to *Faraday's law*

$$u = -w \frac{d\Phi}{dt} \quad (7)$$

( $u$  voltage induced in a coil at change of magnetic flux  $d\Phi/dt$ ,  $w$  number of turns) needs not to be considered. For dynamic simulation, however, split mmf

sources are challenging due to the strong interactions between the electrical and magnetic domain given by *Faraday's* law (Eq. (7)) and *Ampere's* law

$$V_{mag} = i w \quad (8)$$

( $V_{mag}$  magnetic voltage across mmf source,  $i$  current). Eq. (7) and Eq. (8) are implemented in the electromagnetic converters *coil1* and *coil2* of Figure 4b. The parasitic capacitances  $c_{par1}$  and  $c_{par2}$  are required to ensure definite voltages across both halves of the coil. The values of the auxiliary resistors  $R_{par1}$  and  $R_{par2}$  have been chosen so that simulation is numerically stable and fast.

In order to evaluate the accuracy in static and dynamic behaviour to be achieved with the above-mentioned lumped network models, a dynamic model of the example actuator based on more accurate finite element analysis (FEA) has been created as a reference (Figure 5). In this model, one of several possibilities to describe an electromagnetic actuator's dynamic behaviour with look-up tables obtained from stationary FEA is implemented. Here, the actuator force  $F(x, I)$  and the flux linkage  $\psi(x, I)$  were calculated for different fixed armature positions  $x$  and stationary currents  $I$  with FEA. The derived tabular function  $\psi(x, I)$  was inverted to  $I(x, \psi)$  as required in the model. The voltage across the current source  $i_{Coil}$  is according to *Kirchhoff's* voltage law for the actuator's electrical subsystem, which is given by

$$u = iR_{coil} + \frac{d\Psi(x, i)}{dt} \quad (9)$$

( $u$  voltage across coil terminals  $p$  and  $n$ ,  $i$  current,  $R_{coil}$  coil resistance).

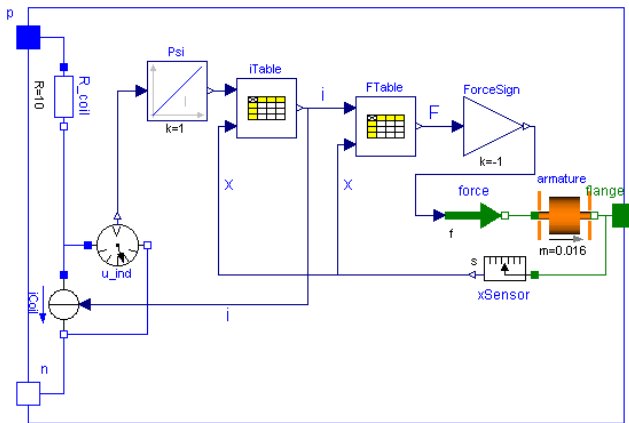


Figure 5: Dynamic model of sample actuator based on look-up tables obtained from stationary FEA

In Figure 6, the accuracy in stationary behaviour to be achieved between the network model of Figure 4, the above-mentioned simple network model without

radial leakage between armature and yoke and the more accurate FEA-based model of Figure 5 is compared. All curves were derived from a quasi-static forced movement of the models armature at a given, constant voltage. The negative sign of the actuator force is due to the definition of the armature coordinate  $x$  which is equal to the length of the working air gap.

The static force-stroke characteristics  $F(x)|_{i=\text{const}}$  of all three models are similar. However, differences between both network models can be observed for the magnetic flux through the armature and for the static inductance  $L_{stat} = \psi/I$ , especially at large air gaps where the leakage permeance  $G_{mLeakRad}$  is large compared to the net permeance  $G_{mAirWork} + G_{mLeakWork}$  of the air gap region. The differences in static inductance between both network models will result in different dynamic behaviour of both models, as Figure 7 indicates.

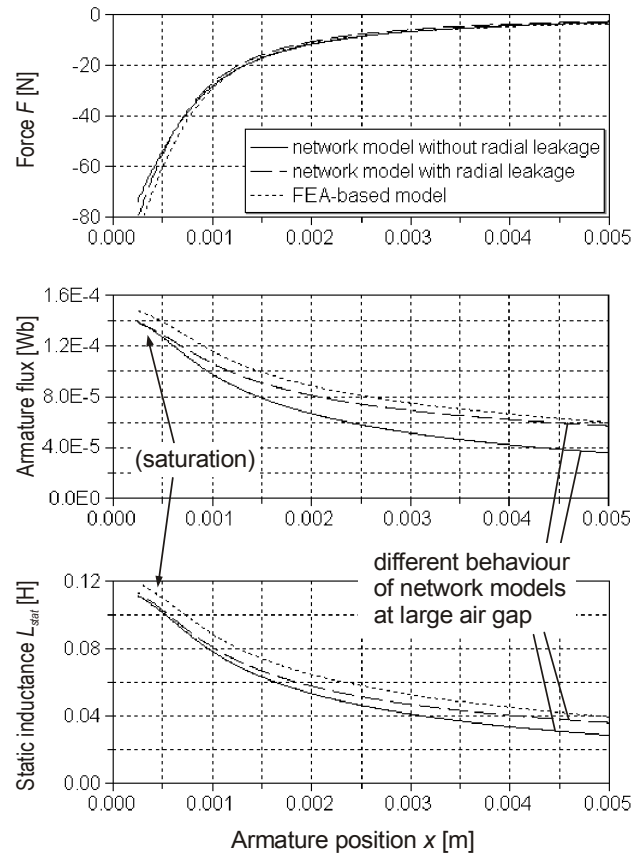


Figure 6: Comparison of stationary behaviour of a simple lumped magnetic network model without radial leakage, the network model of Figure 4b with radial leakage and the FEA-based model of Figure 5

Differences in model behaviour during a simulated pull-in stroke of the armature are shown in Figure 7. At time  $t=0$ , a voltage step is applied to both lumped network models and to the FEA-based model of the

actuator. The characteristic current drop during pull-in is due to the motion-induced emf and to the increase of the inductance with decreasing air gap. One can see that the simulated current rise of the network model with radial leakage is closer to that of the FEA-based reference model than the current rise of the simple network model without radial leakage. As a result, the magnetic force of latter model shows the fastest rise and simulated armature motion is faster than that of the FEA-based model.

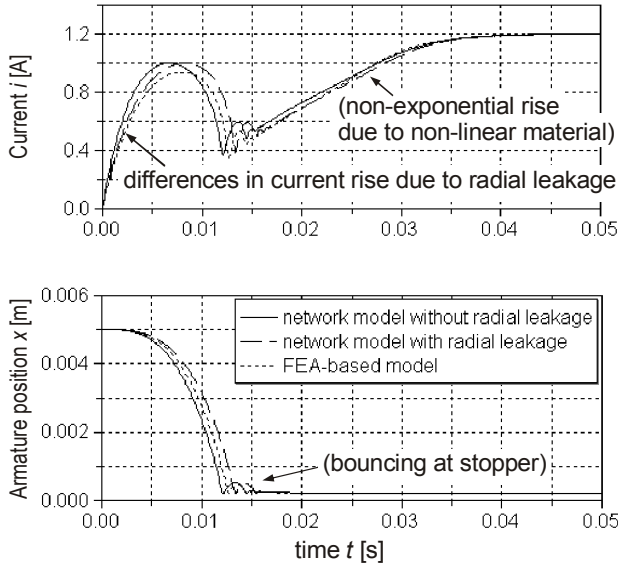


Figure 7: Comparison of the models dynamic behaviour with a simulated pull-in stroke (voltage step applied at time  $t = 0$ )

## 5 Modelling of Electrodynamic Actuators

Similar to the well-known behavioural model of a rotational DC-Machine, the electro-mechanical conversion process of translatory electrodynamic actuators (either moving coil or moving magnet type) can be described with a motor constant  $c_m$ :

$$F_L = c_m i, \tag{10a}$$

$$u_i = c_m v. \tag{10b}$$

$F_L$  denotes the electrodynamic or *Lorentz* force,  $i$  the current,  $u_i$  the induced back-emf and  $v$  the velocity of the armature. During design of such actuators, the motor constant as well as the motor inductance can be determined by means of a lumped magnetic network model of an actuator's magnetic circuit.

As an example, Figure 8a shows the principal structure of an axisymmetric translatory electrodynamic actuator with moving coil. The flux lines and the flux

density of the permanent magnetic field were calculated with FEA as a reference (Figure 8b, half-section). Figure 9 shows a Modelica model of that actuator intended for dimensioning of the actuator's magnetic circuit and winding and for subsequent dynamic simulation at the system level. This example is included as `MagneticCircuitModel` in package `Examples.ElectrodynamicActuator` of the library.

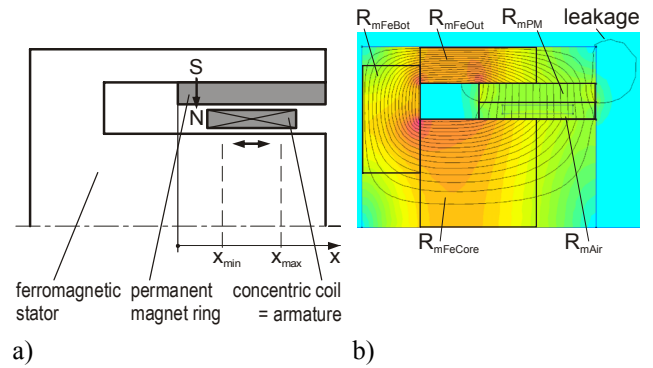


Figure 8: *Translatory electrodynamic actuator*: a) Structure; b) FEA field plot of permanent magnetic field and partitioning into flux tubes

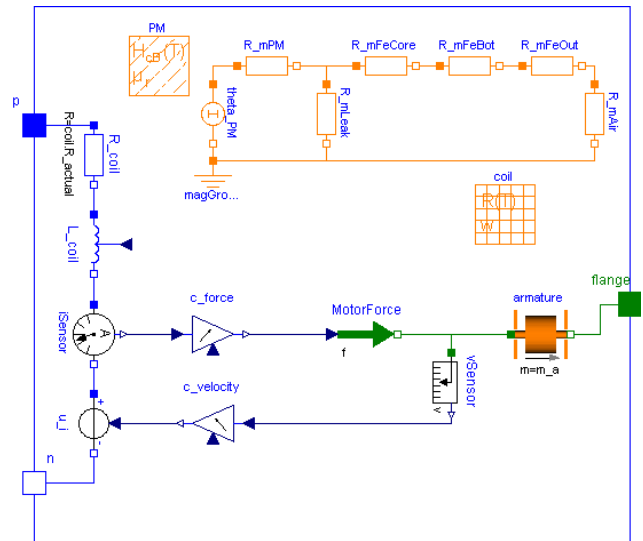


Figure 9: Dynamic model of the electrodynamic actuator of Figure 8 with lumped magnetic network for determination of motor constant and inductance

Although the formula for estimation of the total magnetic reluctance  $R_{m\ tot}$  perceived by the coil is rather simple in this model, comparison with FEA showed that it is well-suited for initial rough design and system simulation of the actuator. The relative difference of the inductance

$$L_{coil} = w^2 / R_{m\ tot} \tag{11}$$

( $w$  number of turns) compared to more accurate FEA is -12% for the armature in mid-position. For useful operating currents, the relative differences of the air gap flux density and the resulting *Lorentz* force to the values obtained with FEA are within -5% to -8%. This accuracy is sufficient for both initial actuator design and system simulation.

## 6 Summary and Outlook

New features and improvements of a Modelica library for lumped network modelling of electromagnetic devices [1] were presented. Two examples, an electromagnetic and an electrodynamic translatory actuator showed that magnetic network models can be used efficiently for the rough design of such devices. These examples are included in the respective sub-packages of the library and can thus be examined in depth.

Despite the simplicity of the presented models, their accuracy is sufficient for preliminary design, as comparisons with more accurate FEA revealed. The dimensions, cross-sections and winding parameters found with magnetic network models can be input data to a subsequent detailed design with FEA or similar techniques, if necessary.

A suitable approach for lumped network modelling of leakage fields for *dynamic* simulation was discussed in detail. Insertion of appropriate leakage permeances into a magnetic network model requires splitting of a devices coil into separate mmf sources. This is challenging due to the multiple couplings between the electrical and the magnetic domain in such a model.

For some electromagnetic devices, lumped network modelling is not possible or reasonable due to distinct leakage fields, complex pole shapes or - with certain actuators - flux tubes and network structures that vary considerably with armature motion. Examples of such devices are inductors without a closed core or proportional solenoids. In this case, dynamic models for system simulation can be created with look-up tables obtained from stationary FEA or similar techniques. One of several possible structures of such a model is shown in section 4.

At present, network modelling of translatory actuators is supported by the library. If needed, the provided model components can be adapted to network modelling of rotational devices. Hysteresis of ferromagnetic materials is currently neglected, since the intention of the library is to support the rough design of electromagnetic devices where a limited accuracy is often sufficient. If necessary, the provided flux

tube elements can be extended so that hysteresis is considered.

It is planned to include the developed library into the Modelica Standard Library after an evaluation period.

## References

- [1] Bödrich, T.: Modelica\_Magnetic library. <http://www.modelica.org/libraries/> (Oct 11, 2007)
- [2] Bödrich, T.; Roschke, T.: A Magnetic Library for Modelica. Proc. of 4th International Modelica Conference, Hamburg, March 7-8, 2005, pp. 559-565
- [3] Roters, H.: Electromagnetic Devices. New York: John Wiley & Sons 1941
- [4] Kallenbach, E.; Eick, R.; Quendt, P.; Ströhla, T.; Feindt, K.; Kallenbach, M.: Elektromagnete: Grundlagen, Berechnung, Entwurf und Anwendung. 2nd ed. Wiesbaden: B.G. Teubner 2003
- [5] Hendershot, J.R. Jr.; Miller, T.J.E.: Design of Brushless Permanent-Magnet Motors. Magna Physics Publishing and Oxford University Press 1994
- [6] Roschke, T.: Entwurf geregelter elektromagnetischer Antriebe für Luftschütze. Fortschr.-Ber. VDI Reihe 21 Nr. 293. Düsseldorf: VDI Verlag 2000